*Journal of Radiation Research*, Vol. 59, No. 6, 2018, pp. 685–691
doi: 10.1093/jrr/rry069
Advance Access Publication: 25 August 2018

# High susceptibility of mouse newborns to delayed appearance of DNA double-strand breaks in neural stem/progenitor cells exposed to ionizing radiation

Kenta Sakaguchi[1,2], Kazunori Shiraishi[1] and Seiji Kodama[1,*]

[1]Laboratory of Radiation Biology, Department of Biological Science, Graduate School of Science, Osaka Prefecture University, 1–2 Gakuen-cho, Naka-ku, Sakai, Osaka 599–8570, Japan
[2]Department of Radiology, Kindai University Hospital, 377-2 Ohnohigashi, Osakasayama, Osaka 589-8511, Japan
*Corresponding author. Laboratory of Radiation Biology, Department of Biological Science, Graduate School of Science, Osaka Prefecture University, 1–2 Gakuen-cho, Naka-ku, Sakai, Osaka 599–8570, Japan. Tel/Fax: +81-72-254-9855; Email: kodama@riast.osakafu-u.ac.jp
(Received 7 June 2018; revised 18 July 2018; editorial decision 21 July 2018)

## ABSTRACT

Fetal brains are known to be extremely sensitive to ionizing radiation, which can induce structural and functional defects in the developing brain. However, there is less data on the effects of radiation on newborn brains. To determine the radiation sensitivity in newborn brains, we determined the number of DNA double-strand breaks (DSBs) appearing at later stage post-irradiation in neural stem/progenitor cells (NSPCs) of mouse newborns <3 days old, and compared it with the numbers of DSBs of fetal, 1-week-neonate, 2-week-neonate, and adult mice. DSBs in the nucleus were quantified by counting the number of foci of phosphorylated histone H2AX (γ-H2AX) in NPSCs using a newly developed computer program. Then, we irradiated 14-day fetuses, newborns <3 days old, 1-week-old neonates, 2-week-old neonates, and 12-week-old adult mice with 2 Gy of X-rays. At 6–7 weeks post-irradiation, the brain tissues isolated from the mice were incubated, and DSBs in the growing neurospheres were counted using a focus-counting program. The delayed appearance of DSBs by X-irradiation was evident in NSPCs derived from newborns <3 days old, as well as in 1-week-old neonates, 2-week-old neonates and adult mice, but not 14-day fetuses, at 6–7 weeks post-irradiation. It was of particular interest that the NSPCs of newborns were 2.5-fold more susceptible than those of adults to radiation-induced delayed appearance of DSBs, indicating that newborns <3 days old are the most vulnerable to the delayed effects of radiation among the mouse groups examined.

**Keywords:** DNA double-strand breaks (DSBs); neural stem/progenitor cells (NSPCs); newborn; delayed effect; ionizing radiation; genomic instability

## INTRODUCTION

Survivors of the atomic bombings of Hiroshima and Nagasaki who were exposed to radiation *in utero* did not show a dose-related increase in chromosome translocations in their lymphocytes when they were examined at ~40 years of age, although their mothers did show such an increase [1]. A similar result was observed in laboratory mice—namely, translocations did not persist in the lymphocytes or bone marrow cells of mice irradiated *in utero* or soon after birth [2]. However, these findings are not generalizable to all irradiation models, since fetal irradiation of rats has been shown to induce persistent chromosome translocations in mammary epithelial cells that are similar to the levels in irradiated adults [3]. Moreover, it was reported that irradiation at different fetal stages resulted in different translocation frequencies in adult mouse thyroid cells [4]. In that study, adult mice that had been irradiated with X-rays at 15.5-day-old fetuses (E15.5) showed a higher translocation frequency than unirradiated adult mice, whereas those who had been irradiated with X-rays at 6.5 days of age showed much lower translocation frequency than E15.5 mice. The authors proposed the following explanation. When stem cells are irradiated before migrating into the niche, damaged cells are eliminated and thus make only a limited contribution to organogenesis. In contrast, when stem cells

are irradiated after migrating into the niche, the damaged cells persist and contribute to organogenesis. These reported findings are of particular interest in terms of the age dependence of radiation carcinogenesis, since it is highly probable that a stem cell containing genetic alterations including chromosomal abnormalities will contribute to initiation leading to development of cancer.

Other rodent studies on the age dependence of radiation carcinogenesis demonstrated that mice in the early postnatal period were more susceptible than fetal and adult mice to the induction of liver, pituitary, ovarian and lung tumors, indicating that various types of newborn tissues are at higher risk of the development of cancers than those of fetal and adult tissues [5–9]. Moreover, recent epidemiological studies demonstrated that radiation exposure from computed tomography (CT) scans in childhood increased the risk of cancers, including brain cancers [10, 11]. The findings reported by animal studies and epidemiological studies suggest that developing tissues in the newborn stage are a critical target for radiation carcinogenesis. However, there remains little evidence concerning the sensitivity to radiation exposure in the newborn stage.

Therefore, in the present study, we studied the radiation sensitivity for induction of delayed DSBs at 6–7 weeks post-irradiation in NSPCs derived from mouse newborns <3 days old and compared the sensitivity with those of fetal, neonate (1-week and 2-week-old) and adult mice. The results indicated that newborns <3 days old were most sensitive to the induction of delayed DSBs, suggesting that there exists an age-related difference in sensitivity to the delayed effects of radiation during neuronal development.

## MATERIALS AND METHODS

### Isolation and culture of neural stem/progenitor cells

Primary neural stem/progenitor cells (NSPCs) were isolated from the cerebra of B6C3F1 mice and C57BL/6N mice (Japan SLC; Hamamatsu, Japan) using an enzymatic dissociation kit (StemCell Technologies, Vancouver, BC, Canada). The care and use of animals in this study complied with the relevant laws and institutional guidelines for animal welfare at Osaka Prefecture University. For isolation of mouse NSPCs, the striata or the brain tissues of the subventricular zone were minced using a pair of scissors until no large pieces remained, and incubated in the dissociation solution for 7 min at 37°C, followed by treatment with the inhibition solution. The cell suspension was centrifuged at 1200 rpm for 5 min at room temperature, and the cell pellet was washed three times with the resuspension solution. Then, the cells were cultured in DMEM/Ham's F-12 medium (Nacalai Tesque, Kyoto, Japan) supplemented with 2% B-27 (Thermo Fisher Scientific, Waltham, MA), 20 ng/ml basic fibroblast growth factor (bFGF) (PeproTech, Rocky Hill, CT), 20 ng/ml epidermal growth factor (EGF) (PeproTech), 2 μg/ml heparin sodium salt, and 1% penicillin–streptomycin (Nacalai Tesque) as floating neurospheres at 37°C under humidified 5% $CO_2$ conditions.

### Immunofluorescent staining of γ-H2AX foci

To detect γ-H2AX foci in the nuclei of NSPCs, neurospheres containing NSPCs were dissociated with accutase (Nacalai Tesque), plated on coverslips precoated with 5% poly-L-ornithine hydrobromide (Sigma-Aldrich, St Louis, MO), and incubated for 3 h. The cells on coverslips were fixed with 4% paraformaldehyde phosphate buffer solution (Nacalai Tesque) at room temperature for 15 min, washed with phosphate buffered saline without magnesium and calcium ions (PBS (–)),, permeabilized with 0.5% triton-X (Sigma-Aldrich) in PBS (–) on ice for 5 min, and washed three times with PBS (–). Fixed cells were soaked with a blocking buffer containing 5% Blocking One (Nacalai Tesque) and 0.1% Tween 20 in PBS (–) for 1 h at room temperature. Blocked cells were incubated with an anti-phospho-histone H2AX (Ser139) mouse monoclonal antibody conjugated with Alexa Fluor 488 (1:50; BioLegend, San Diego, CA) for 1 h at room temperature, and then washed three times with 0.5% Tween 20 in PBS (–). The coverslips were mounted with Vectashield mounting medium with DAPI (Vector Laboratories, Burlingame, CA). The edges of each coverslip were sealed with clear nail polish.

### Development of a computer program for counting γ-H2AX foci

Fluorescence of γ-H2AX foci was observed by a fluorescence microscope (BX-51; Olympus, Japan) and photographed using a digital camera (DP71; Olympus). To count the number of γ-H2AX foci accurately and reproducibly, we developed a new computer program. 3D-images instead of 2D-images of the foci were acquired in a movie format by moving the microscope stage along the axis perpendicular to the image plane. The 3D-images consisted of twenty-one 2D-images that were captured from the top to the bottom of a cell over 3 s in AVI format. These pictures were obtained using a microscope equipped with an objective lens of ×100 magnification, and one picture consisted of 1360 × 1024 pixels with a pixel size of 0.065 μm. To acquire high-contrast images, a region of interest (ROI) was placed on the background area as a black balance.

### Evaluation of the focus-counting program

NSPCs isolated from fetuses (14 days of gestation) of ICR mice (Japan SLC) were used for the evaluation of the focus-counting program. After incubation for 3 h on 5% poly-L-ornithine–coated coverslips, the cells were irradiated with 0.5, 1.0, 1.5 and 2.0 Gy of X-rays using an X-ray machine (OM-B205; Ohmic, Tokyo, Japan) operated at 70 kVp and 5 mA using a 0.5 mm Al filter at a dose rate of 0.66 Gy/min at room temperature and cultured at 37°C under humidified 5% $CO_2$ conditions for 30 min. After immunofluorescent staining, the number of γ-H2AX foci was scored by both visual examination and the focus-counting program.

### Detection of DSBs in the NSPCs of irradiated mice

B6C3F1 and C57BL/6N mice were used to measure the delayed appearance of DSBs induced by 2 Gy of X-rays in NSPCs as shown in Fig. 1. B6C3F1 mice were divided into five groups: UY, unirradiated young mice (6 weeks of age); IF, fetuses irradiated at 14 days of gestation; IN-0, newborns irradiated at <3 days of age; IN-1, neonates irradiated at 1 week of age; IN-2, neonates irradiated at 2 weeks of age. In addition, two groups of C57BL/6N adult female mice were included: UA, unirradiated adults (12 weeks old); IA, adults irradiated at 12 weeks of age. The mice of the IF group were sacrificed

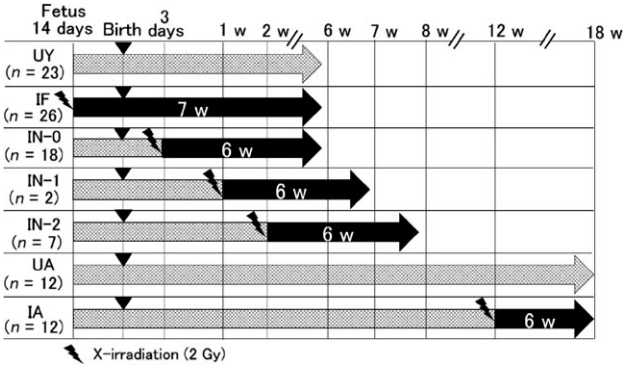


**Fig. 1. Experimental design for detection of DSBs in NSPCs of irradiated mice. B6C3F1 mice were divided into five groups: UY, unirradiated young mice (6 weeks old); IF, fetuses irradiated at 14 days of gestation; IN-0, newborns irradiated at less than 3 days of age; IN-1, neonates irradiated at 1 week of age; IN-2, neonates irradiated at 2 weeks of age. C57BL/6N adult female mice were divided into two groups: UA, unirradiated adults (12 weeks old); IA, adults irradiated at 12 weeks of age. The mice were irradiated with 2 Gy of X-rays for the irradiated groups and examined for detection of DSBs in NSPCs at 6 or 7 weeks post-irradiation. The number of mice used is represented in parentheses.**

for isolation of NSPCs at 6 weeks of age (7 weeks post-irradiation), and the other irradiated mice were sacrificed at 6 weeks post-irradiation. The unirradiated mice of the UY and UA groups were sacrificed at 6 weeks and 18 weeks of age, respectively (Fig. 1). In addition, some of the mice, groups IF, IN-0 and IA, were sacrificed for isolation of NSPCs at 48 h post-irradiation. Mice were irradiated with 2 Gy of X-rays using an X-ray machine (Radioflex-350; Rigaku Denki, Tokyo, Japan) operated at 260 kVp and 12 mA with a 0.3 mm-Cu and 0.5 mm-Al filter at a dose rate of 0.5 Gy/min at room temperature. The irradiated dose (2 Gy) was selected by referring to the former studies [2–4]. Growing neurospheres isolated from mice were subject to immunofluorescent staining for γ-H2AX foci as described above, and the number of the foci were determined using the focus-counting program.

### Statistics

Statistical significance was tested by the Kruskal–Wallis test. *P*-values $< 0.001$ were considered to indicate statistically significant differences.

## RESULTS

### Development of an Image-J based computer program for counting γ-H2AX foci

The number of γ-H2AX foci was quantified using a computer program that we developed based on Image-J; Image-J is an image analyzing program with an open architecture with extensibility using Java plugins. The program consists of four steps as shown in Fig. 2: (1) identification of each nucleus; (2) enhancement of focus intensity; (3) exclusion of noise; (4) calculation of signals. Negative numbers, if acquired, were replaced with zero in all steps. For identification of each nucleus (Step 1), 3D-images were projected into a 2D-image. The command 'Gaussian blur with radius 2.00' was applied to the 2D-images, followed by the following commands: 'make binary', 'unsharp mask (radius = 0.50, mask = 0.90)', 'erode (three times)', 'dilate (ten times)', 'erode (three times)', and 'watershed'. Then, the command 'analyze particles' outputted the individual numbers, sizes, and coordinates of the identified nucleus. Each recognized nucleus was cropped from the original 3D-images according to the corresponding coordinates and sizes. For the enhancement of focus intensity (Step 2), a cropped nucleus was processed sequentially by the commands 'unsharp mask (radius = 10, mask = 0.50)', '3D blur filter', and '3D edge filter'. For exclusion of noise (Step 3), the ROI was placed on a nucleus and the threshold value was determined using the following equation:

$$\text{Threshold value} = \text{average intensity in the ROI} + 2 \times \text{SD (SD, standard deviation)}$$

The 3D-images were binarized using the threshold value and further processed by sequential use of the commands 'erode', 'dilate' and 'watershed' in order to exclude pulse noises, resulting in recognition as foci. Finally, for the calculation of signals (Step 4), the connected-component labeling with 6-connectivity for 3D-images was applied.

### Evaluation of the focus-counting program

The results obtained by our new program for counting γ-H2AX foci indicated that the number of foci increased in a dose-dependent manner, as shown in Fig. 3. For comparison, we determined the number of foci by visual examination and compared the result with that obtained by the computer program (Fig. 3). Linear regression formulae applying the number of the foci per nucleus were as follows:

$$\text{Focus-counting program: } 7.20\ D(\text{Gy}) + 0.42 (r^2 = 0.998)$$
$$\text{Visual examination: } 7.61\ D(\text{Gy}) + 0.38 (r^2 = 0.988)$$

As shown in Fig. 3, the numbers of foci per nucleus obtained by the program were very similar to those scored by the visual examination. Thus, the focus-counting program would be expected to provide good reproducibility and a minimum variance in quantifying the number of DSBs in nuclei. Therefore, we decided to use this program to quantify the delayed appearance of DSBs induced by X-irradiation in NSPCs.

### Delayed appearance of DSBs induced by X-irradiation in NSPCs

As shown in Fig. 1, we attempted to quantify the DSBs appearing in mouse NSPCs at 6 or 7 weeks post-irradiation. In particular, we were interested in the delayed appearance of DSBs in NSPCs of fetuses and newborns, because the developing brain was hypersensitive to radiation. For the unirradiated condition, the mean numbers of γ-H2AX foci per nucleus of young (UY; 6-week-old) and adult

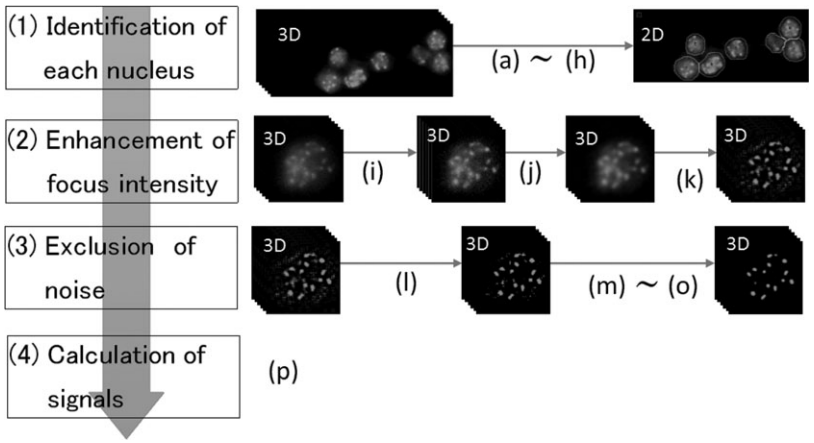


**Fig. 2. Image-processing procedures for the computer program for counting γ-H2AX foci. The program consists of four steps: (1) identification of each nucleus; (2) enhancement of focus intensity; (3) exclusion of noise; (4) calculation of signals. Each step contained the following commands. (a) Gaussian blur with radius 2.00; (b) make binary; (c) unsharp mask; (d) erode; (e) dilate; (f) erode; (g) watershed; (h) analyze particle; (i) unsharp mask; (j) 3D blur filter; (k) 3D edge filter; (l) threshold; (m) erode; (n) dilate; (o) watershed; (p) connected-component labeling with 6-connectivity for 3D-images.**

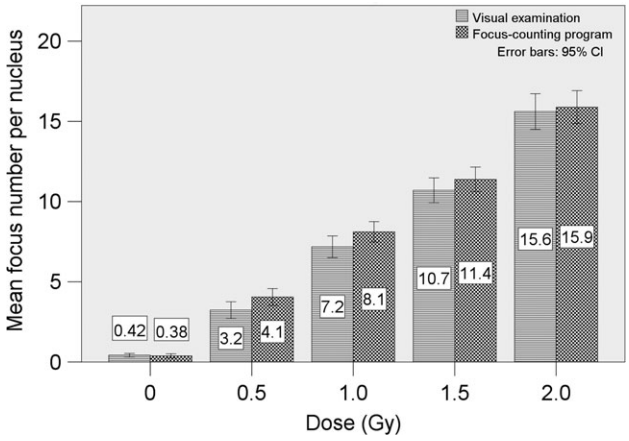


**Fig. 3. Dose–response relationship between the number of γ-H2AX foci and graded doses. The results obtained using the computer program were represented as compared with those obtained by the visual examination. The numbers in each column represent the mean of the focus numbers per nucleus. The number of cells analyzed was 188–232 per dose for each method. Error bars represent 95% confidence intervals.**

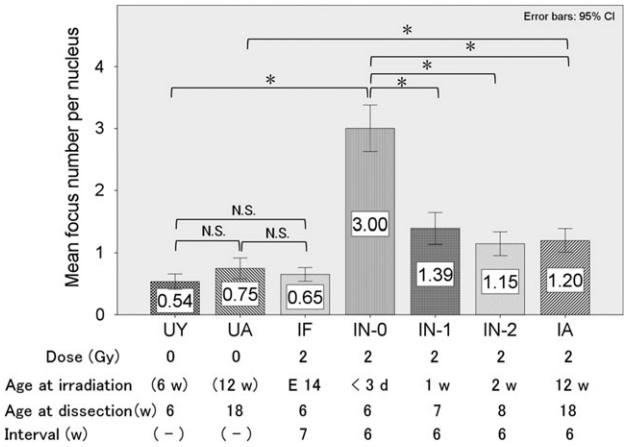


**Fig. 4. Delayed appearance of DSBs in NSPCs of mice exposed to X-irradiation. The mice were examined for detection of DSBs in NSPCs at 6 or 7 weeks post-irradiation. After isolation from the mice, neurospheres were cultured for almost 2 weeks and then fixed for immunostaining. The number of γ-H2AX foci was determined using the focus-counting program. UY, unirradiated young mice (6 weeks old); IF, fetuses irradiated at 14 days in gestation; IN-0, newborns irradiated at <3 days of age; IN-1, neonates irradiated at 1 week of age; IN-2, neonates irradiated at 2 weeks of age; UA, unirradiated adults (12 weeks old); IA, adults irradiated at 12 weeks of age. The number of cells analyzed was 420–700 per group. Error bars represent 95% confidence intervals. Statistical significance was tested by the Kruskal–Wallis test. *$P < 0.001$ was considered to be a statistically significant difference. N.S., not significant.**

(UA; 18-week-old) mice were 0.54 and 0.75, respectively, and the difference was not significant (Fig. 4). The mean number of the foci of irradiated fetuses (IF) was 0.65, which was not significantly different from those of unirradiated young (UY) and adult (UA) mice, indicating that the delayed appearance of DSBs by X-irradiation was not evident in NSPCs derived from 14-day-old fetuses (Fig. 4). In contrast, the mean focus numbers in irradiated newborns <3 days

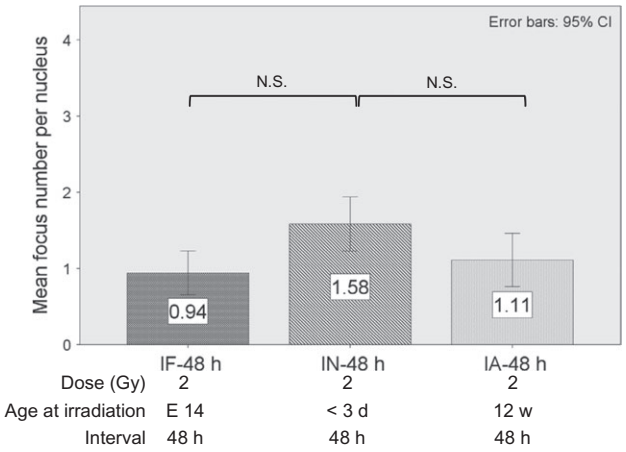


**Fig. 5. Appearance of DSBs in NSPCs of mice at 48 h post-irradiation. The mice were examined for detection of DSBs in NSPCs at 48 h post-irradiation. After isolation from the mice, neurospheres were cultured for almost 2 weeks and then fixed for immunostaining. The number of γ-H2AX foci was determined using the focus-counting program. IF-48 h, fetuses irradiated at 14 days in gestation; IN-48 h, newborns irradiated at <3 days of age; IA-48 h, adults irradiated at 12 weeks of age. The cell numbers analyzed for IF-48 h, IN-48 h and IA-48 h were 68 cells, 273 cells and 161 cells, respectively. Error bars represent 95% confidence intervals. Statistical significance was tested by the Kruskal–Wallis test. *$P < 0.001$ was considered to be a statistically significant difference. N.S., not significant.**

old (IN-0) and in adult mice (IA, 18 weeks old) were significantly higher than those in unirradiated young (UY) and adult mice (UA), respectively (Fig. 4). Moreover, the average focus number in NSPCs of newborns (IN-0), 3.00 per nucleus, was 2.5-fold greater than that of adult mice (IA), 1.20 per nucleus, indicating that NSPCs of newborns (IN-0) were most sensitive to induction of the delayed appearance of DSBs. On the other hand, the mean focus numbers of neonates irradiated at 1 week old (IN-1: 1.39) and those irradiated at 2 weeks old (IN-2: 1.15) were much lower than those of newborns (IN-0: 3.00), and thus the levels were similar to those of irradiated adult mice (IA: 1.20).

To determine the effect of X-rays (2 Gy) on the appearance of delayed DSBs for periods <6–7 weeks, we determined the number of γ-H2AX foci in NSPCs of mice at 48 h post-irradiation (Fig. 5). The examined mice were 14-day-old fetuses (IF-48 h), newborns <3 days of age (IN-48 h) and adults (IA-48 h; 12 weeks old). As shown in Fig. 5, the results revealed that the mean focus numbers per nucleus of fetuses, newborns, and adults were 0.94, 1.58 and 1.11; the NSPCs of newborns tended to be the most sensitive, although there were no statistically significant differences between the three groups. This meant that the delayed DSBs appearing at 6 weeks post-irradiation were not those retained in nuclei of NSPCs but rather those newly emerged in growing NSPCs as neurospheres in culture.

## DISCUSSION

In the present study, we developed an Image-J-based automated program for counting γ-H2AX foci and demonstrated that the program provided rapid, accurate and reproducible quantification of the focus numbers. We then used the program to improve the large variance in the focus numbers among scorers, which has been a major disadvantage of visually performed focus evaluations. The evaluation of γ-H2AX foci existing on a cross section of a nucleus may result in underestimation because the foci existing out of focus in the section are not targets for evaluation. To count all foci existing 3-dimensionally in a nucleus, a common approach of the automated focus-counting program reported in the previous papers was superimposing 2D-images at different cross-sections of a nucleus [12–16]. However, those approaches still contained uncertainty, including counting loss by the overlap of signals and counting false positive signals caused by the sum of noise. In contrast to this, the most improved characteristics of our approach was that we captured 3D-images from the top to the bottom of a cell in a movie format and reconstructed a 3D-image composed of twenty-one 2D-images instead of superimposing 2D-images. By evaluating the number of foci in the reconstructed 3D-image, we succeeded in reducing the counting loss due to the signal overlaps and false positive signals. As shown in Fig. 3, the results obtained by the computer program indicated that the number of the foci increased linearly depending on the dose up to 2 Gy, and the dose–response relation was closely correlated with that obtained by the visual examination, resulting in similar linear regression formulae. In addition, other data including integrated fluorescence intensity, average fluorescence intensity, and average focus size are also available. Taken together, these results indicate that the present focus-counting program is practically suitable for evaluating the number of DSBs in irradiated cells, and further enables us to identify differences in sensitivity to the delayed appearance of DSBs between mice at different ages.

Of particular interest, when NSPCs were collected from the mice of 6 weeks old irradiated at <3 days of age and grown as neurospheres in culture, they showed an increased number of DSBs. This is the first report indicating that NSPCs of newborns (<3 days old) are highly susceptible to a delayed, radiation-induced appearance of DSBs. In our previous report, we showed that the number of X-ray–induced DSBs in NSPCs of 14-day-old fetuses decreased in a time-dependent manner from 1 h to 12 h after irradiation to the level of unirradiated NSPCs when the cells were irradiated *in vitro* [17]. It is reasonable to consider that the kinetics of DSB repair *in vitro* reflect the kinetics occurring *in vivo*. Therefore, it is not likely that the DSBs that emerged in growing neurospheres post-irradiation were derived from the DSBs produced at the time of irradiation. This interpretation was supported by our observation that the numbers of DSBs induced by X-irradiation in NSPCs were significantly different between fetuses, newborns and adult mice at 6–7 weeks post-irradiation, but not at 48 h post-irradiation. Morphology of γ-H2AX foci appearing at 6–7 weeks post-irradiation was very similar to that of those that appeared 48 h post-irradiation. Therefore, we suggest that the DSBs newly appeared during the growth phase of NSPCs in culture, because DSBs, once produced, will strictly activate the cell cycle checkpoint, inducing a

strong growth arrest of NSPCs [18]. Thus, the present study suggests that NSPCs of newborn mice within 3 days of birth are susceptible to radiation-induced genomic instability, which leads to the production of DSBs in later stages of brain development. Although the mechanism by which radiation induces genomic instability was not clarified in the present study, an earlier report concerning the delayed appearance of DSBs in germ cells of male mice exposed to ionizing radiation is worthy of consideration. Namely, Cordelli *et al.* [19] reported that spermatogonia produced spermatids harboring DSBs 33 and 45 days after irradiation, although radiation-induced DSBs were repaired within 2 h in testicular cells, demonstrating that non-targeted DNA lesions appeared in the descendants derived from radiation-surviving spermatogonia. They suggested that proliferating spermatogonia retained some memory of the radiation exposure that activated a process leading to DSBs at a later stage of development. Further, they proposed that DNA synthesis in proliferating spermatogonia might predispose the DNA damage-response machinery to leave a mark of lesion processing at the sites of DNA damage. Further interpretation of their findings could suggest a mechanism for the delayed appearance of DSBs observed in the present study.

The former rodent studies demonstrated that mice exposed to radiation *in utero* or soon after birth showed lower or similar frequencies of chromosome translocations in lymphocytes, mammary epithelial cells, and thyroid cells compared with adult mice exposed to radiation [2–4]. In contrast to those studies, we here demonstrated that newborns <3 days old, but not fetuses and neonates (1 week and 2 weeks old), were highly (2.5-fold more) sensitive to the delayed appearance of DSBs by X-irradiation in NSPCs compared with adult mice. This high sensitivity to radiation exposure in newborns was also reported in a human cytogenetic study [20]. The authors of that study irradiated lymphocytes of umbilical cord blood derived from newborns and those from adults *in vitro* and found that newborns were significantly more sensitive to radiation-induced structural chromosome aberrations than adults. This is in contrast to the findings reported by Ohtaki *et al.* [1], who observed that human fetuses exposed to ionizing radiation from the atomic bombs did not show increased frequencies of chromosome translocations in their lymphocytes. Therefore, both animal and human studies suggest that a change in sensitivity to radiation occurs between fetuses and newborns.

Finally, it is notable that a similar age dependence of susceptibility has been demonstrated in rodent studies on radiation carcinogenesis [5–9]. The essential finding of those studies is that newborn mice are more susceptible than fetal and adult mice to the induction of various types of tumors by radiation exposure. In particular, it is noteworthy that our results indicate the appearance of DSBs in growing NSPCs, which can differentiate into various neural progenitors. Because radiation carcinogenesis is presumed to be a multistep process, the accumulation of multiple gene mutations should be required in addition to the initial DNA damage by radiation. During carcinogenesis, genetic instability can play a crucial role in the accumulation of gene mutations, including chromosome aberrations [21, 22]. Therefore, the fact that irradiation to newborns (<3 days old) induces genomic instability that leads to the production of DSBs in the later stage of brain development is important in terms of the increased risk of brain tumors due to radiation exposure in childhood. In this context, it is worth noting that epidemiological studies demonstrated that radiation exposure from computed tomography (CT) scans in childhood increased the risk of cancers, including brain tumors [10, 11]. We suggest that the increased sensitivity to the emergence of delayed DSBs at the newborn stage by radiation contributes to the increase in cancer risk associated with radiation exposure in childhood.

In summary, by developing a new computer program for evaluating DSB numbers, we measured the number of DSBs in growing mouse NSPCs derived from fetuses, newborns <3 days old, 1-week-old neonates, 2-week-old neonates, and adults (12 weeks old) at 6–7 weeks post-irradiation and found that newborns <3 days old showed the highest rate of delayed appearance of DSBs in NSPCs after irradiation. The present findings should contribute to future risk assessment for ionizing radiation exposure. Further studies will be needed to clarify the mechanism of the change in sensitivity to radiation-induced delayed appearance of DSBs between fetuses and newborns.

## ACKNOWLEDGEMENTS

The authors thank Dr Hiroki Kashiwagi and Mr Yosuke Shirasaka for their technical advice and helpful discussions, and Miss Maki Fukui for technical assistance.

## CONFLICT OF INTEREST

The authors declare that there are no conflicts of interest.

## FUNDING

This work was supported by the Japan Society for the Promotion of Science (JSPS) KAKENHI [Grant Numbers JP26550032 and JP16K12599].

## REFERENCES

1. Ohtaki K, Kodama Y, Nakano M et al. Human fetuses do not register chromosome damage inflicted by radiation exposure in lymphoid precursor cells except for a small but significant effect at low doses. *Radiat Res* 2004;161:373–9.
2. Nakano M, Kodama Y, Ohtaki K et al. Chromosome aberrations do not persist in the lymphocytes or bone marrow cells of mice irradiated *in utero* or soon after birth. *Radiat Res* 2007;167:693–702.
3. Nakano M, Nishimura M, Hamasaki K et al. Fetal irradiation of rats induces persistent translocations in mammary epithelial cells similar to the level after adult irradiation, but not in hematolymphoid cells. *Radiat Res* 2014;181:172–6.
4. Hamasaki K, Landes RD, Noda A et al. Irradiation at different fetal stages results in different translocation frequencies in adult mouse thyroid cells. *Radiat Res* 2016;186:360–6.
5. Sasaki S. Influence of the age of mice at exposure to radiation on life-shortening and carcinogenesis. *J Radiat Res* 1991;32:73–85.
6. Sasaki S, Fukuda N. Dose–response relationship for induction of solid tumors in female B6C3F1 mice irradiated neonatally with a single dose of gamma rays. *J Radiat Res* 1999;40:229–41.

7. Sasaki S, Fukuda N. Dose–response relationship for lifetime excess mortality and temporal pattern of manifestation in mice irradiated neonatally with gamma rays. *J Radiat Res* 2002;43:313–23.
8. Sasaki S, Fukuda N. Temporal variation of excess mortality rate from solid tumors in mice irradiated at various ages with gamma rays. *J Radiat Res* 2005;46:1–19.
9. Hattis D, Goble R, Russ A et al. Age-related differences in susceptibility to carcinogenesis: a quantitative analysis of empirical animal bioassay data. *Environ Health Perspect* 2004;112:1152–8.
10. Pearce MS, Salotti JA, Little MP et al. Radiation exposure from CT scans in childhood and subsequent risk of leukaemia and brain tumours: a retrospective cohort study. *Lancet* 2012;380: 499–505.
11. Mathews JD, Forsythe AV, Brady Z et al. Cancer risk in 680,000 people exposed to computed tomography scans in childhood or adolescence: data linkage study of 11 million Australians. *BMJ* 2013;346:f2360.
12. Runge R, Hiemann R, Wendisch M et al. Fully automated interpretation of ionizing radiation–induced gammaH2AX foci by the novel pattern recognition system AKLIDES(R). *Int J Radiat Biol* 2012;88:439–47.
13. Cai Z, Vallis KA, Reilly RM. Computational analysis of the number, area and density of gamma-H2AX foci in breast cancer cells exposed to $^{111}$In-DTPA-hEGF or gamma-rays using Image-J software. *Int J Radiat Biol* 2009;85:262–71.
14. Bocker W, Iliakis G. Computational methods for analysis of foci: validation for radiation-induced gamma-H2AX foci in human cells. *Radiat Res* 2006;165:113–24.
15. Hernandez L, Terradas M, Martin M et al. Highly sensitive automated method for DNA damage assessment: gamma-H2AX foci counting and cell cycle sorting. *Int J Mol Sci* 2013;14: 15810–26.
16. Barber PR, Locke RJ, Pierce GP et al. Gamma-H2AX foci counting: image processing and control software for high-content screening. *Proc SPIE* 2007;6441:64411M-1–10.
17. Kashiwagi H, Shiraishi K, Sakaguchi K et al. Repair kinetics of DNA double-strand breaks and incidence of apoptosis in mouse neural stem/progenitor cells and their differentiated neurons exposed to ionizing radiation. *J Radiat Res* 2018;59: 261–71.
18. Huang L-C, Clarkin KC, Wahl GM. Sensitivity and selectivity of the DNA damage sensor responsibile for activating p53-dependent G1 arrest. *Proc Natl Acad Sci U S A* 1996;93: 4827–32.
19. Cordelli E, Eleuteri P, Grollino MG et al. Direct and delayed X-ray–induced DNA damage in male mouse germ cells. *Environ Mol Mutagen* 2012;53:429–39.
20. Bakhmutsky MV, Joiner MC, Jones TB et al. Differences in cytogenetic sensitivity to ionizing radiation in newborns and adults. *Radiat Res* 2014;181:605–16.
21. Teixeira da Costa L, Lengauer C. Exploring and exploiting instability. *Cancer Biol Ther* 2002;1:212–25.
22. Tomasetti C, Vogelstein B, Parmigiani G. Half or more of the somatic mutations in cancers of self-renewing tissues originate prior to tumor initiation. *Proc Natl Acad Sci U S A* 2013;110: 1999–2004.